EPJ Photovoltaics **14**, 6 (2023)

https://doi.org/10.1051/epjpv/2022032

**Special Issue on 'WCPEC-8: State of the Art and Developments in Photovoltaics', edited by Alessandra Scognamiglio, Robert Kenny, Shuzi Hayase and Arno Smets**

Available online at: www.epj-pv.org

REGULAR ARTICLE

OPEN ACCESS

# Energy performance of commercial c-Si PV modules in accordance with IEC 61853-1, -2 and impact on the annual specific yield

Christos Monokroussos[1,*], Yating Zhang[1], Eleanor W. Lee[2], Frank Xu[1], Allen Zhou[1], Yichi Zhang[1], and Werner Herrmann[3]

[1] TÜV Rheinland (Shanghai) Co., Ltd., No. 177, Lane 777, West Guangzhong, 200072 Shanghai, P.R. China
[2] TÜV Rheinland Taiwan Ltd., 11F., No. 758, Sec. 4, Bade Rd., Songshan Dist., Taipei 105, Taiwan
[3] TÜV Rheinland Energie und Umwelt GmbH, Am Grauen Stein, 51105 Cologne, Germany

Received: 27 June 2022 / Received in final form: 1 November 2022 / Accepted: 9 December 2022

**Abstract.** As energy yields of photovoltaic modules are highly related to local climate and ambient conditions, it is necessary to assess the energy-yield performance of PV modules under various operating conditions. This work compares commercial crystalline silicon (c-Si) based PV modules (including mono c-Si Al BSF, mono c-Si PERC, multi-crystalline (mc-Si) Al BSF, and n-type c-Si solar cells) sampled from 27 PV module manufacturers located in the Asia-Pacific region between 2016 and 2022. Several test items were compared including: (i) light-induced degradation (LID), (ii) irradiance-temperature-efficiency (GTE) matrix, (iii) angular response and (iv) temperature coefficients, which are correspondingly performed according to IEC 61215-1, -1-1, -2 and IEC 61853-1, -2. The coefficient of variation (CoV) was calculated to express the module-to-module differences within similar technology types. Benefiting from the technological innovation of c-Si based PV modules, emerging PV modules feature better performance in some extreme ambient conditions, such as low irradiance, high ambient temperature, and high ratio of diffuse irradiance. The analysis of CoV indicates that the difference of irradiance-dependent and thermal behavior between modules within the same technology may exceed the differences between different technologies. Using synthetic hourly meteorological data of 5 sites from MeteoNorm in PVsyst, the annual specific yield of four technology groups of PV modules were simulated and compared. Overall, it is shown that the maximum differences as large as 7.34% in terms of PV module's specific yield are expected within same PV technology, which exceeds the maximum difference of 2.16% obtained for specific yields of different PV technologies.

**Keywords:** Energy performance / silicon-based PV modules / LID / angular response / temperature coefficient / GTE matrix / IEC 61853-1,-2 / PVsyst

## 1 Introduction

By the end of 2021, the global cumulative PV installed capacity has amounted to at least 942 GW, which stays in a constantly growth stage [1]. Along with the rapid development of the PV industry, plenty of innovative technologies continue to rise, such as the emerging innovative materials and structures aiming of harvesting more solar energy [2–6]. To compare and evaluate different PV technologies and module types, the power (watts) rating of PV modules was provided and relevant measurement methods were investigated. In the early stage of PV industry, the rating of photovoltaic (PV) modules is only carried out under standard test conditions (STC, 25 °C device temperature, and irradiance of 1000 W/m$^2$ with the reference spectral irradiance distribution as defined in IEC 60904-3) [7]. The STC rating also has a significant economic impact on the PV industry, because it determines the price of each module. However, PV modules operate and yield energy over a much broader range of irradiance and temperature under realistic weather conditions [8–10]. This has led to misconceptions where PV modules were priced based on their power rating under STC, and not their ability to produce units of electricity outdoors [11]. In response, the IEC TC82 proposed the IEC 61853 series of standards [12–15]. IEC 61853-1, -2 describe requirements for a holistic characterization of PV module performance under various operating conditions and defines the methodology to determine the energy (watts-hours) output and energy rating of PV modules

* e-mail: Christos.Monokroussos@tuv.com

with standard reference climatic profiles. To be more specific, in IEC 61853-1 are described the test procedures to evaluate the irradiance and temperature behaviors of PV modules through power rating measurements over a range of irradiances and temperatures; all the procedures to account for the effects affecting the module performances such as angle of incidence, module operating temperature and spectral effects are described separately in IEC 61853-2. IEC 61853-3 provides a methodology for the energy rating calculation using the climatic profiles defined in IEC 61853-4.

To further evaluate the energy performance of PV modules in a power plant, a software, PVsyst, is commonly used to design and model the PV system at a specific location [16,17]. A reliable database of PV modules performance data guarantees an accurate yield forecast. The database usually includes STC performance, irradiance-dependent behavior, angular response, temperature dependence, and LID of PV modules, and the procedures for these performance measurements follow the ones described in IEC 61853 series standards. Energy yield can be calculated taking into consideration the target meteorological data, the technology of the PV modules, and the components used in the PV system.

A characterization comparison of mono and multi crystalline silicon (c-Si) PV modules according to IEC 61853 has been previously presented in [18]. In this work, the comparison is extended to more commercial c-Si based PV module types based on new available data. This work compares the characterizations of crystalline silicon based PV modules (including mono c-Si Al BSF, mono c-Si PERC, mc-Si Al BSF, and n-type c-Si solar cells) sampled from 27 PV module manufacturers located in the Asia-Pacific region between 2016 and 2022. In addition, encapsulated solar cells coming from the same batch and with the same bill of materials of the PV modules under test were used for the measurement of the spectral response. The test specimens were subsequently transported for testing to the ISO/IEC 17025 accredited PV laboratory of TÜV Rheinland in Shanghai. Initially all PV modules were verified to meet the requirements of IEC 61215-1 for visual defects [18], and electroluminescence (EL) imaging was performed for all modules to make sure all samples were in good condition. Prior to their characterization in accordance with IEC 61853-1, -2, PV modules were electrically stabilized in accordance with IEC 61215-1, -1-1, and -2 standards [19–21]. The test items to be reported in this work are (i) light-induced degradation (LID), (ii) irradiance-temperature-efficiency (GTE) matrix, (iii) angular response and (iv) temperature coefficients. It is noted that the nominal module operating temperature (NMOT) test has not been performed in this work. Moreover, the annual specific energy yields of four types of PV modules were compared based on PVsyst simulation. This paper shows that PV module characterization under IEC 61853 is critical and can lead to a paradigm shift of the industry's practices. The calculated maximum differences in terms of PV modules specific energy yield within the same PV technology were observed to be larger than the differences calculated for different PV technologies.

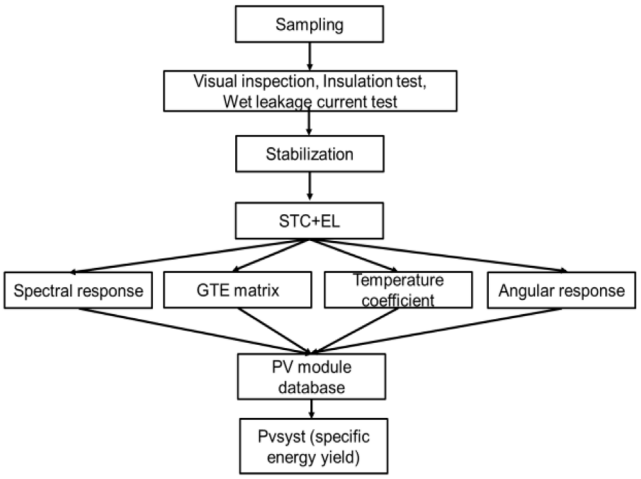


**Fig. 1.** The test and simulation flow used for calculation of energy yield.

## 2 Methodology

### 2.1 Module characterization

In this work, nearly 100 module types from 27 PV module manufacturers located in the Asia-Pacific region between 2016 and 2022 were cataloged into four groups: (i) mono c-Si Al BSF types, (ii) mc-Si Al BSF types, (iii) mono c-Si PERC types, (iv) n-type c-Si types which includes n-type c-Si, Heterojunction Technology (HJT) and Tunnel Oxide Passivate Contact Technology (TOPCon). For analyzing the influence of technology innovation on PV energy performance, the PV modules within one group were additionally separated according to the manufacturing year. For each PV module type, 4 full-sized PV modules were sampled from production by independent engineers. Additionally, one encapsulated solar cell coming from the same batch and with the same bill of materials of the test PV module was needed to determine the spectral response of the test specimen. The PV modules are reported here anonymously to ensure the confidentiality of all parties involved.

All the tests were carried out by the ISO/IEC 17025 accredited PV laboratory of TÜV Rheinland in Shanghai. For this PV laboratory, the measurement uncertainty of power rating under STC was less than $\pm 2.0\%$ ($k = 2$), which was specifically estimated according to the principles detailed in the "Guide to the expression of uncertainty in measurement" (GUM) [22]. The test flow of this work was illustrated in Figure 1. Initially, the PV modules were subject to the visual inspection, insulation test, and wet leakage test according to IEC 61215-1, -1-1, -2 [18–20] to approve the basic design qualification of the test specimens; then the PV modules were electrically stabilized prior to the electrical characterization. In addition, an electroluminescence imaging (EL) test was performed, which showed that all the test specimens were in good condition. After these initial tests, the modules went through a series of tests in accordance with IEC 61853-1,-2. The tests include (i) light-induced degradation (4 full-sized samples per

**Table 1.** Summary of test sites and abstract information used in specific energy yield comparison.

| Site | Coordinates | PV module elevation [m] | PV module tilt | Global Irrad. [kWh/m$^2$] | Diffuse Irrad. [kWh/m$^2$] | Mean temp. [°C] |
|---|---|---|---|---|---|---|
| Chennai, India | 13°N, 80.18°E | 66 | 15° | 1941.8 | 942.8 | 28.2 |
| Cologne-Bonn, Germany | 50.7°N, 7.15°E | 1067 | 38° | 979 | 544.6 | 11 |
| DaTong, China | 40.1°N, 113.3°E | 755 | 38° | 1480.9 | 670.4 | 8 |
| Riyadh, Saudi Arabia | 24.91°N, 46.41°E | 19 | 27° | 2189.2 | 649.2 | 26.4 |
| Rio de Janeiro, Brazil | –22.9°N, –43.2°E | 10 | 23° | 1690.5 | 840.7 | 23.9 |

type); (ii) irradiance-temperature-efficiency (GTE) matrix (3 full-sized samples per type); (iii) spectral response (1 encapsulated solar cell sample with the same bill of materials of each module type); (iv) angular response (1 full-sized sample per module type); (v) temperature coefficient, TC (1 full-sized sample per module type). All the performance characterization results mentioned above were recorded in a database, which was utilized as an input for PVsyst modeling. Using the meteorological data of the five locations reported in Table 1, the specific energy yield of each PV module type was calculated at each location and compared.

A class BBA+ (B class spectrum, B class non-uniformity, and A+ class long-term temporal instability) steady-state solar simulator was used for the stabilization of PV modules prior to their characterization. During the stabilization, the temperature of the DUT was kept within $55 \pm 5$ °C. A pulsed solar simulator of class A+A+A+ was used to perform all power rating measurements including STC measurement, GTE matrix, TC and angular response. The irradiance of the solar simulator was monitored by a primary reference cell, which was calibrated at periodic intervals to a secondary standard at Physikalisch-Technische Bundesanstalt (PTB). Different intensity of irradiance was achieved by using optical meshes, which do not alter the spectral distribution. The test was carried out in a thermostatic room, and a temperature control system was applied to adjust the temperature to meet the requirements of GTE and TC measurements. Under this system, the temperature of the reference cell and tested PV module were controlled within ±0.5 °C. The spectral response of all PV modules were measured according to IEC 60904-8 [23] and utilized to calculate the spectral mismatch factor for the power rating measurements [24]. Temperature and irradiance corrections of the measured $I$–$V$ data were carried out according to the procedures defined in IEC 60891 [25].

For the angular response measurement, a rotatable open rack was employed with a ball-point rotating unit mounted on a calibrated goniometer. The equivalent optical distance between the test sample and the light source was approximately 8 m. PV modules under test were specially prepared by accessing directly the electrical terminations of the measured solar cell located in the middle of the PV module to confine the non-uniformity of irradiance variation on the volume of rotation of the target cell. The non-uniformity of irradiance reached 0.6% in the test plane and 1.9% on the volume of rotation of the test cell. Three successive baffle layers were employed to suppress the diffuse light and to restrict the irradiance on the test plane within a field of view of 20°. An anti-reflective black painting was used on the walls to eliminate secondary reflections.

### 2.2 Energy yield simulation

To comprehensively quantify the effects of the performances of the PV modules, the specific energy yield was calculated based on PVsyst software. The validation of energy yield simulations for PV modules with PVsyst software was performed in previous work [26–28]. In this work, the electrical performance data of each PV module type was obtained from the measurements performed at the TÜV Rheinland laboratory in Shanghai. Five test sites that represent different climates were chosen: (i) Chennai in India with a tropical wet and dry climate, (ii) Cologne-Bonn in Germany with a temperate oceanic climate, (iii) DaTong in China with a continental monsoon-influenced steppe climate, (iv) Riyadh in Saudi Arabia with a long desert climate, and (v) Rio de Janeiro in the Brazil with a tropical savanna climate. A summary of the selected sites, their climatic conditions and mounting tilt is shown in Table 1. The hourly meteorological data of these five sites were synthesized through MeteoNorm embedded in PVsyst software. As the aim of this work was to compare the specific yield between different module types operated at certain sites, the uncertainty of the Meteonorm insolation data used would not significantly impact the relative comparison. It should be noted that inverter sizing losses were kept below 0.1% in the simulation. Wind effects on the thermal behavior of PV modules in the field were neglected, while a heat transfer coefficient of 20 W/m$^2\cdot$K was used as a default setting. Bifaciality and additional losses such as soiling or annual degradation were not considered in the simulation.

## 3 Results and discussion

### 3.1 Light-induced degradation

Light-induced degradation (LID) refers to a performance and power loss of solar cells due to the excess carrier injection by illumination or forward biasing [29,30]. Most industrial c-Si solar cells and modules are suffering from some type of LID. Even a 1% drop in power will result in considerable energy and capital losses. The LID

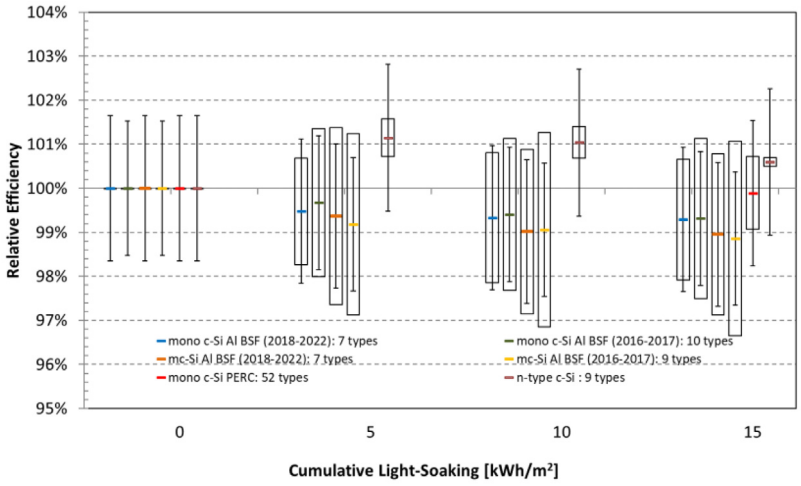


**Fig. 2.** Light-induced degradation (LID) expressed as relative efficiency (to initial) against cumulative irradiation dose for different module types at STC. Boxes represent the standard deviation of technology variation ($k = 2$) and error bars represent the measurement uncertainty ($k = 2$).

phenomenon has been studied for four decades since it was first observed in Czochralski-grown c-Si devices in the 1970s [31]. Several LID degradation types have been observed such as boron-oxygen complex activation (BO-LID), Copper-related (Cu-LID), iron-boron pair dissociation (FeB-LID) and mc-PERC LID [32–34], however, the specific responsible recombination-active defects were not yet identified [35]. Among these degradation types, BO-LID is the mostly recognized degradation effect, which is usually observed in clean boron-doped Cz-Si. In recent years, gallium has been introduced as a dopant instead of boron, which results in lower LID losses. The Cz-Si with interstitial copper suffers from the Cu-LID regardless of concentrations of other elements [36,37]. While mc-Si solar cells show less degradation compared to the similarly doped Cz-Si solar cells in consideration of the less oxygen and higher carbon concentration. Some mc-Si solar cells may also exhibit more detrimental degradation, as the copper contamination is induced by the process of mc-Si wafer crystallization. In addition, mc-Si with rear passivated (mc-PERC) shows an unexpected strong degradation and this mc-PERC LID is prone to occur at high temperatures [38]. In contrast to the degradation caused by light exposure, the relative efficiency increase appears in HJT solar cells with doped a-Si:H/c-Si structures under light soaking [39].

In accordance with IEC 61215-1, -1-1, and -2 standards, all test PV modules were electrically stabilized before any further measurement. The results of relative efficiency (to initial) against cumulative irradiation dose for different module types at STC are illustrated in Figure 2. The relative efficiency losses of all PV modules due to LID stays within 3.5% after light soaking of 15 kWh/m$^2$. No obvious difference in LID loss was observed for c-Si and mc-Si PV modules manufactured in different years. Mono c-Si Al BSF, mc-Si Al BSF, and mono c-Si PERC samples showed an average LID of 0.70%, 1.10%, and 0.11% respectively. N-type c-Si samples, the majority of which are HJT technologies with n-type Cz-Si wafer, showed an average 0.60% relative efficiency increase. The standard deviation within technology groups was calculated as coefficient of variation (CoV) in this work. It is worth noting that the module-to-module variation within certain technology was more significant than the difference between different technology types except for n-type c-Si types, with CoV = 1.37%, $k = 2$ for mono c-Si Al-BSF types (2016–2017), CoV = 1.81%, $k = 2$ for mono c-Si Al BSF types (2018–2022), CoV = 1.83%, $k = 2$ for mc-Si Al BSF types (2016–2017), CoV = 2.21%, $k = 2$ for mc-Si Al BSF types (2018–2022), CoV = 0.83%, $k = 2$ for mono c-Si PERC types and CoV = 0.10%, $k = 2$ for n-type c-Si types. This indicates that even for similar technology types, large dispersion would exist due to both wafer quality and manufacturing processes employed.

### 3.2 Effect of irradiance on module performance

Irradiance and temperature are two key factors that affect the energy yield of PV modules in the field. IEC 61853-1 provides a matrix of module performance with respect to temperature and irradiance as a useful tool to characterize the different irradiance and thermal behavior of the PV module. The following typical irradiance and temperature values are selected in this matrix: (1) 100, 200, 400, 600, 800, 1000 and 1100 W/m$^2$; (2) 15 °C, 25 °C, 50 °C and 75 °C [12]. The irradiance-depended performance is highly related to the PV module technology. Figure 3 shows the comparison of the efficiency relative to STC of different PV module types.

The results showed that the relative efficiency losses associated with low irradiances below 400 W/m$^2$ were observed for all PV types, however, there was no significant variation of relative efficiency with respect to their STC performance in the range of 600–1100 W/m$^2$. This efficiency loss towards low light is mainly attributed to the shunt resistance, series resistance and diode quality factor [40].

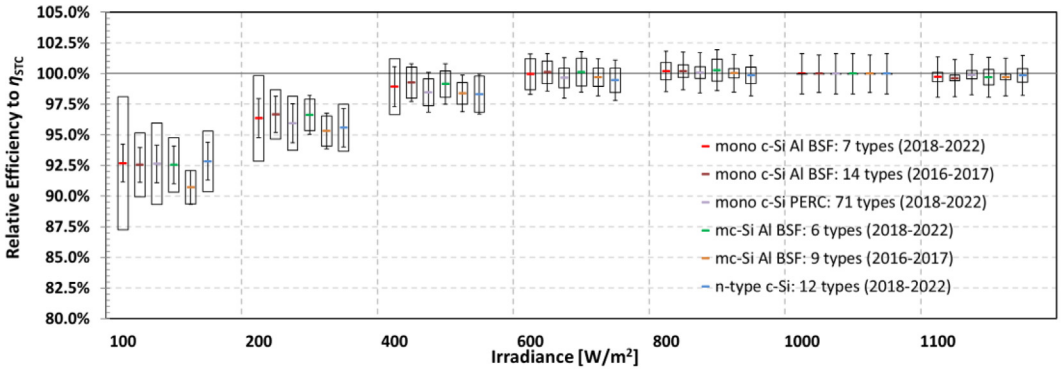


**Fig. 3.** Relative efficiency deviation (to STC) against irradiance for different module types at 25 °C and spectral distribution of AM1.5G. Boxes represent the standard deviation of technology variation ($k = 2$) and error bars represent the measurement uncertainty ($k = 2$).

For the irradiance below 400 W/m$^2$, the comparative relation in relative efficiency loss between different PV module types differed slightly per irradiance level. However, the mc-Si Al BSF samples (2016–2017) were the most noticeably affected, with an efficiency drop of 9% at the irradiance of 100 W/m$^2$, while the other technology types showed an average relative efficiency loss of around 7%. Due to the technology improvement of mc-Si passivation, the performance of mc-Si Al BSF samples at low irradiance has improved (shown in mc-Si Al BSF (2018–2022)). The use of low-resistivity wafers, which have been recently introduced may worsen the relative performance of the samples at low-irradiance, which can be seen in the large relative efficiency variation (5.43%, $k = 2$) observed for mono c-Si Al BSF samples (2018–2022) for irradiance of 100 W/m$^2$. The performance for mono c-Si Al BSF and mc-Si Al BSF samples in the range of 600–800 W/m$^2$ was relatively higher than STC, which is attributed to the lower losses over the series resistance of the PV module. Furthermore, the variability in the relative efficiency of PV modules within the same technology group can be significant specifically for the low irradiances. The CoV exceeded the bounds of relative measurement uncertainty for all technology types, with CoV varying from 1.37%, $k = 2$ for mc-Si Al BSF (2016–2017) to CoV = 5.43%, $k = 2$ for mono c-Si Al BSF (2018–2022) at 100 W/m$^2$.

### 3.3 Effect of temperature on module performance

Thermal behavior plays an important role in the performance of solar cells and their energy output, which decreases with increasing operating temperature. This is because the internal carrier recombination is accelerated under enhanced carrier concentrations [41]. A photovoltaic (PV) module in the field is rarely working at the same condition as STC. Most of the incident solar energy which fails to be converted into electricity, and dissipates as heat, leading to an increased module temperature and worsened performance. For silicon-based PV modules, a linear dependency of both the electrical performance and the power output on the operating temperature is expected.

In accordance with IEC 60891, the temperature coefficients, $\alpha$ of $I_{SC}$, $\beta$ of $V_{OC,}$ and $\delta$ of $P_{MAX}$, for all PV module types were measured and shown in Figure 4. Among three temperature coefficients, the temperature coefficient of $P_{MAX}$ was most sensitive to the variability of PV technologies. The mean temperature coefficients for mono c-Si Al BSF (2018–2022), mono c-Si Al BSF (2016–2017), mc-Si Al BSF (2018–2022), mc-Si Al BSF (2016–2017), mono c-Si PERC and n-type were approximately $-0.388\% \cdot K^{-1}$, $-0.407\% \cdot K^{-1}$, $-0.403\% \cdot K^{-1}$, $-0.398\% \cdot K^{-1}$, $-0.343\% \cdot K^{-1}$ and $-0.346\% \cdot K^{-1}$, respectively.

The mean temperature coefficients of $I_{SC}$, $V_{OC,}$ and $P_{MAX}$ were approximately equal for mono c-Si Al BSF and mc-Si Al BSF module types excluding the case of mono c-Si Al BSF (2018–2022) which contained only three PV modules. In comparison with mono c-Si and mc-Si types with Al-BSF, a slight difference in the temperature coefficient of $I_{SC}$ was observed for mono c-Si PERC and n-type c-Si PV modules. On the other hand, mono c-Si PERC and n-type c-Si PV modules showed a lower absolute value of mean temperature coefficients of $V_{OC}$ and $P_{MAX}$, which indicates that the temperature increase will result in less power loss for these PV modules. It is then possible to state that the technology type is responsible for the reduced temperature coefficients of $V_{OC}$ and $P_{MAX}$. It is known that high-efficiency solar cells, i.e. PERC and HJT, with higher Voc, which can be achieved by reduced surface and bulk recombination, will result in a reduced temperature dependency of $V_{OC}$ and $P_{MAX}$ [42].

### 3.4 Incident angular response

The incident light striking on the surface of PV modules is partially reflected back or absorbed by the materials composing the front cover, such as glass or EVA, or the $SiN_x$. Only a portion of it will finally hit the solar cells. These optical losses vary per incidence angle. The PV module performance varying with the angle of incidence (AoI, the angle between the beam irradiation and the normal to the surface of PV modules) is defined as its angular response. Typically the STC power measurement

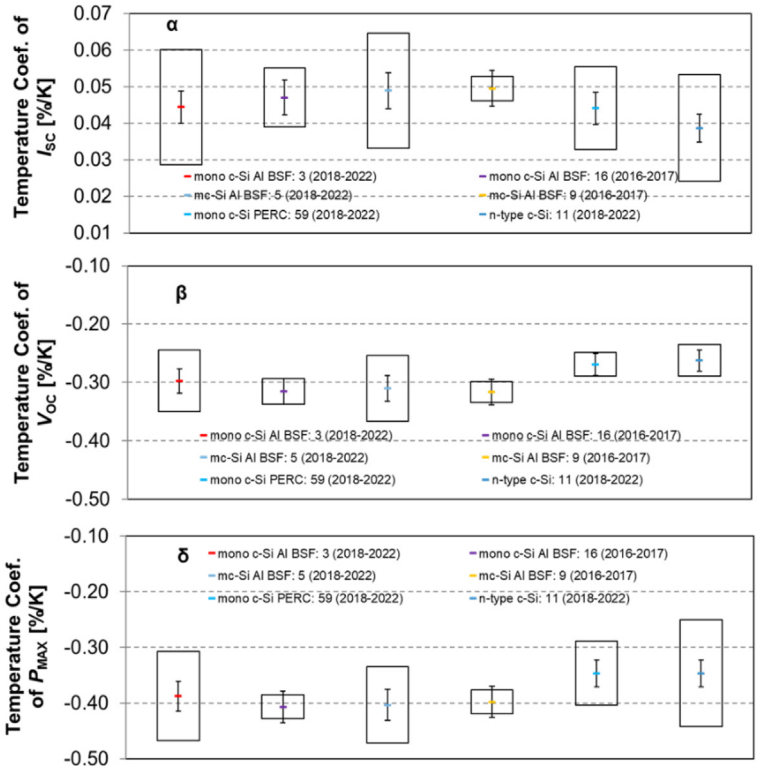


**Fig. 4.** Temperature coefficients of $I_{SC}$, $V_{OC}$, and $P_{MAX}$ for different module types. Boxes represent the standard deviation of technology variation ($k=2$) and error bars represent the measurement uncertainty ($k=2$). Differences overlap with the uncertainty in measurement.

is performed in laboratories with solar simulators that have strong specular components [22], thus most of the irradiation will be normal to the front surface of PV modules. When operating outdoors, however, PV modules are subject to diffuse angular profiles that may introduce significant optical losses. The power annual losses due to incidence angle effects may be typically in the order at least 3% for PV systems [43]. To quantify the incidence angle effects on flat-plate PV modules, the test methodology is defined in IEC 61853-2.

The $I_{SC}$ values measured at different incident angles for several PV modules were translated into the relative transmission according to IEC 61853-2 and the results are presented in Figure 5. The results of angular response for different module types were cataloged by the manufacture year, and the largest deviations were observed at oblique angles exceeding 50°. Due to the continued optimization of properties of the textured surface and anti-reflection coatings of the front cover, PV modules manufactured between 2018 and 2022 featured better light harvesting, especially for the light with large incident angles. The measurement uncertainty and CoV for each incident angle had strong angular dependences. For incident angles larger than 50°, the CoV of two groups of PV modules increase strongly. This indicates that the relative transmission at larger incident angles was more prone to be affected by the properties of lamination materials. Meanwhile, the module-to-module variation within group 2018–2022 spread farther out, specifically with the CoV at 80° corresponding to 5.42%, $k=2$ and 7%, $k=2$ for groups 2016–2017 and 2018–2022.

### 3.5 Energy yield comparison

Energy yield represents the capacity of power generation of PV modules and arrays, and it is affected by the installing location, seasonal and year-to-year variations. Based on this concept, specific energy yield is further proposed, and it specifically refers to how much energy (kWh) is produced for every kWp. The specific energy yield is commonly used to compare the performances of PV systems installed at different locations or of different PV system designs. In this work, annual specific energy yields of four PV module types at five different sites were simulated using PVsyst. As the outdoor spectral irradiance data were not available in PVsyst, the outdoor spectral mismatch effect is not taken into account. The error in relative annual energy yield differences caused by the spectral effects was less than 2% due to the similarity in spectral responsivity of c-Si PV [10,44].

As shown in Figure 6 for each site, the mean annual yields of mono c-Si and mc-Si were approximated as equal, while mono c-Si PERC and n-type samples consisting of HJT and TOPCon, PV modules produced more annual specific yield. The relative difference between the maximum and minimum mean yield per site varied within 0.73%

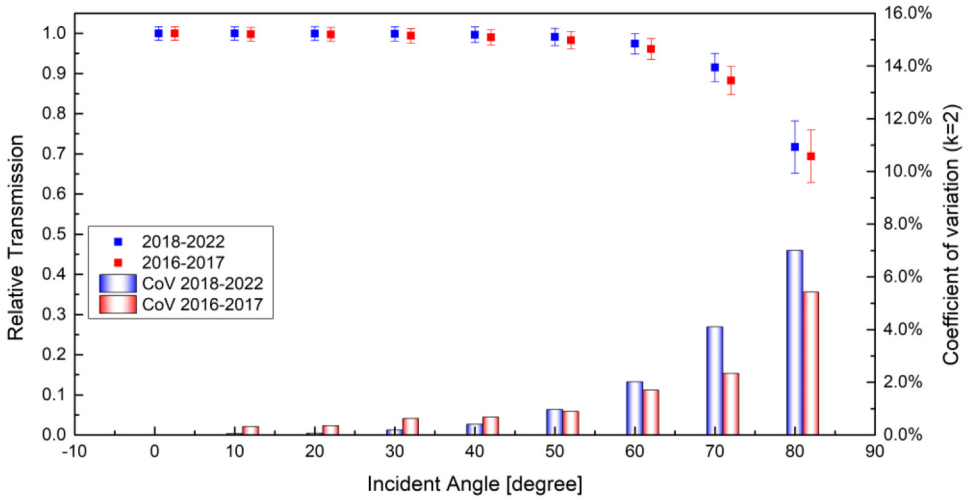


**Fig. 5.** Variation of relative angular transmission for PV modules manufactured in different years. Bars represent the standard deviation of technology variation ($k = 2$).

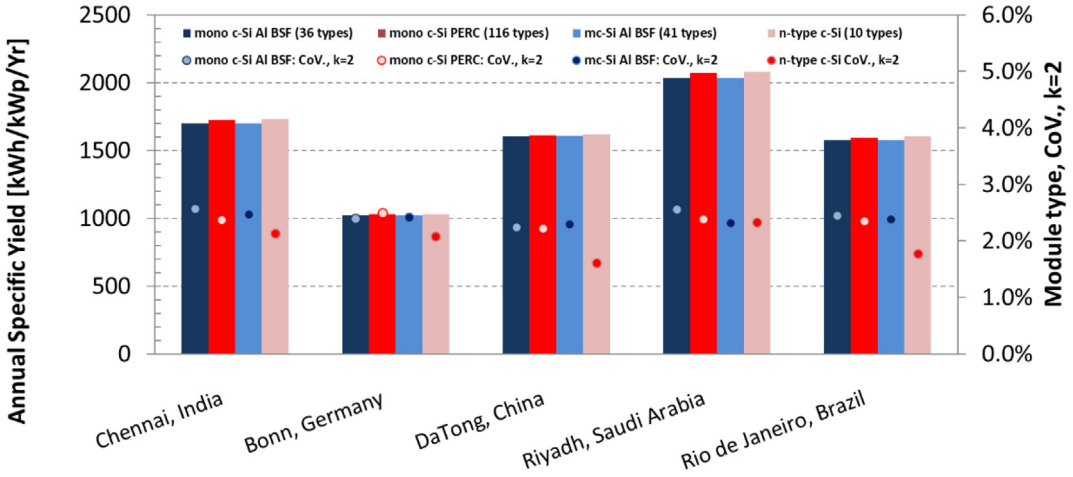


**Fig. 6.** Variation of specific energy yield over 5 sites and coefficient of variation for 4 module types. Bars represent the annual specific yield and dots the coefficient of variation of specific yield from type to type ($k = 2$).

(Datong, China) to 2.21% (Riyadh, Saudi Arabia). For c-Si PERC Al BSF and n-type PV modules, the specific energy yield boost mainly benefits from the better behavior at low irradiances, high temperature, or incident light with large angles. CoV of mono c-Si Al BSF, mono c-Si PERC and mc-Si Al BSF PV modules varied approximately within 2.23% to 2.57% ($k = 2$), while the CoV for n-type c-Si PV samples varied more widely within 1.61% (DaTong, China) to 2.33% (Riyadh, Saudi Arabia). This indicates that energy yields of n-type c-Si PV modules are more sensitive to the factors such as insolation conditions, local climate, and surrounding environment. Among PV modules within same PV technology, the maximum difference in terms of PV module's specific yield for one site was 7.34%, which exceeds the relevant differences of 2.16% between different PV technologies.

## 4 Conclusions

IEC 61853 standard series is aiming at assessing various aspects of PV module performance that affect PV energy yield forecast. This work was initiated with the purpose of evaluating the performance of commercial mainstream silicon-based PV modules according to IEC 61853, specifically in terms of spectral response, light-induced degradation, irradiance dependent behavior, thermal behavior, and angular response. Measured data of modules from 27 PV module manufacturers located in the Asia-Pacific region between 2016 and 2022 were collected and compared. The analysis was based on the coefficient of variation (CoV), calculated to express the module-to-module differences.

In LID tests, the relative efficiency losses of all PV module types stayed within 3.5% after light soaking of 15 kWh/m$^2$; the polycrystalline samples were found more susceptible to LID, with an average LID loss of 1.10% after light soaking of 15 kWh/m$^2$; the n-type samples exhibited an efficiency increase after light soaking. The coefficient of variation also indicated that the variation of LID losses may vary more within module types than technology types.

At low irradiance (<400 W/m$^2$), minor differences were observed in the performance between different PV module types. Due to technology development, the mean relative efficiency deviation to STC of mc-Si Al BSF PV modules increased from 90.72% (2016–2017) to 92.56% (2018–2022) at irradiance of 100 W/m$^2$. Comparing modules of similar PV technology such as for mono c-Si Al BSF (2016–2017), it was found that the variation in terms of relative efficiency reduction between different modules became more significant at lower irradiance; the CoV decreases from 5.43% ($k=2$) to 1.26% ($k=2$) along with irradiance increasing from 100 W/m$^2$ to 600 W/m$^2$.

The sensitivity of temperature coefficients to module variability is not particularly significant for $I_{SC}$, $V_{OC,}$ and $P_{MAX}$ for both mono c-Si Al BSF and mc-Si Al BSF PV samples. Due to the reduced recombination of high-efficiency solar cells, mono c-Si PERC and n-type samples have shown smaller temperature dependency on $V_{OC}$ and $P_{MAX}$ compared to mono c-Si and mc-Si samples.

PV modules manufactured between 2018 and 2022 feature better light harvesting compared to samples manufactured between 2016 and 2017, especially at large incident angles above 60°.

Lastly, calculations of specific energy yield in 5 different sites were carried out based on the results of above-mentioned measurements for different module types. Generally, it was found that the high-efficiency PV modules which mainly include PERC, HJT, and TOPCon PV modules have higher energy yield compared to mono c-Si and mc-Si modules with Al BSF. The maximum PV module specific relative differences as large as 7.34% were observed between crystalline-based PV modules within same technology, while the maximum difference between different PV technologies was found to be within 3%.

## Author contribution statement

Christos Monokroussos, main author. Yating Zhang, helped in writing the article and also data analysis. Frank Xu, helped with measurements and data analysis. Eleanor Lee, helped with data analysis. Allen Zhou, performed most measurements. Yichi Zhang, supported by dedicating lab resources and lab equipment to us. Werner Herrmann, several helpful discussions and comments.

## References


1. Snapshot of Global Photovoltaic Markets 2022. Report IEA PVPS T1-42 (2022)
2. M.D. Udayakumar, G. Anushree, J. Sathyaraj, A. Manjunathan, Mater. Today: Proc. **45**, 2053 (2021)
3. M. Giannouli, Int. J. Photoenergy **2021**, 6692858 (2021)
4. D.B. Mesquita et al., in *Proceedings of the IEEE PES Innovative Smart Grid Technologies Conference-Latin America* (2019)
5. H. Schulte-Huxel et al., Sol. Energy Mater. Sol. Cells **200**, 109991 (2019)
6. F. Gerenton et al., in *Proceedings of IEEE 46th Photovoltaic Specialists Conference (PVSC)* (2019), http://doi.org/10.1109/PVSC40753.2019.8981179
7. IEC 60904-3: 2016, Photovoltaic devices – Part 3, Measurement principles for terrestrial photovoltaic (PV) solar devices with reference spectral irradiance data (2016)
8. R. Lad, J. Wohlgemuth, G. TamizhMani, in *Proceedings of IEEE Photovoltaic Specialists Conference (PVSC)* (2010), https://doi.org/10.1109/PVSC.2010.5616859
9. D. Dirnberger, B. Müller, C. Reise, Prog. Photovolt. Res. Appl. **23**, 1754 (2015)
10. M. Schweiger, W. Herrmann, A. Gerber, U. Rau, IET Renew. Power Gener. **11**, 558 (2017)
11. M. Schweiger, W. Herrmann, in *Proceedings of 31st European Photovoltaic Solar Energy Conference and Exhibition, Hamburg* (2015)
12. IEC 61853-1: 2011, Photovoltaic (PV) module performance testing and energy rating – Part 1: Irradiance and temperature performance measurements and power rating (2011)
13. IEC 61853-2: 2016, Photovoltaic (PV) module performance testing and energy rating – Part 2: Spectral responsivity, incidence angle and module operating temperature measurements (2016)
14. IEC 61853-3: 2018, Photovoltaic (PV) module performance testing and energy rating – Part 3: Energy rating of PV modules (2018)
15. IEC 61853-4: 2018, 2015, Photovoltaic (PV) module performance testing and energy rating – Part 4: Standard reference climatic profiles (2018)
16. K.J. Sauer, T. Roessler, C.W. Hansen, IEEE J. Photovolt. **5**, 01 (2015)
17. Y.M. Irwan et al., Energy Procedia **79**, 604 (2015)
18. C. Monokroussos et al., in *Proceedings of 33rd European Photovoltaic Solar Energy Conference and Exhibition, Amsterdam* (2017)
19. IEC 61215-1: 2016, Terrestrial photovoltaic (PV) modules – Design qualification and type approval –Part 1: Test requirements (2016)
20. IEC 61215-1-1: 1: 2016, Terrestrial photovoltaic (PV) modules – Design qualification and type approval –Part 1-1: Special requirements for testing of crystalline silicon photovoltaic (PV) modules (2016)
21. IEC 61215-2: 2016, Terrestrial photovoltaic (PV) modules – Design qualification and type approval – Part 2: Test procedures (2016)
22. Evaluation of Measurement Data – Guide to the Expression of Uncertainty in Measurement. JCGM 100 (2008)
23. IEC 6090 4-8:2014, Photovoltaic devices – Part 8: Measurement of spectral responsivity of a photovoltaic (PV) device (2014)
24. IEC 6090 4-7:2019, Photovoltaic devices – Part 7: Computation of the spectral mismatch correction for measurements of photovoltaic devices (2019)
25. IEC 60891: 2009, Photovoltaic devices – Procedures for temperature and irradiance corrections to measured I-V characteristics (2009)
26. A. Mermoud, Note about the PHOTON simulation software survey (2011)

27. B. Wittmer, A. Mermoud, T. Schott, in *Proceedings of 30th European Photovoltaic Solar Energy Conference and Exhibition, Hamburg* (2015)
28. J.B. Castro, M. Herz; C. Monokroussos, M. Schweiger, in *Proceedings of 35th European Photovoltaic Solar Energy Conference and Exhibition, Brussels* (2018)
29. H. Hashigami, Y. Itakura, T. Saitoh, J. Appl. Phys. **93**, 7 (2003)
30. J. Knobloch, S.W. Glunz, in *Proceedings of 25th IEEE Photovoltaic Specialists Conference* (1996), pp. 405–408
31. R.L. Crabb, in *Proceedings of 9th IEEE Photovoltaic Specialists Conference, Silver Springs, MD, USA* (IEEE, 1972), pp. 243–249
32. B. Sopori, P. Basnyat, S. Devayajanam, S. Shet, V. Mehta, J. Binns, J. Appel, in *Proceedings of 2012 IEEE Photovoltaic Specialists Conference, Austin* (2012)
33. T. Luka, C. Hagendorf, M. Turek, Photovolt. Int. **32**, 37 (2016)
34. K. Ramspeck, S. Zimmermann, H. Nagel, A. Metz, Y. Gassenbauer, B. Birkmann, A. Seidl, in *Proceedings of 27th European Photovoltaic Solar Energy Conference and Exhibition, Frankfurt* (2012)
35. J. Lindroos, H, Savin, Sol. Energy Mater. Sol. Cells **147**, 115 (2016)
36. H. Savin, M. Yli-Koski, A. Haarahiltunen, Appl. Phys. Lett. **95**, 152111 (2009)
37. J. Lindroos et al., Phys. Status Solidi Rapid Res. Lett. **7**, 262 (2013)
38. K. Ramspeck et al., in *Proceedings of the 27th European Photovoltaic Solar Energy Conference and Exhibition*, Frankfurt (2012), pp. 861–865
39. E. Kobayashi et al., Appl. Phys. Lett. **109**, 153503 (2016)
40. P. Grunow, S. Lust, D. Sauter, V. Hoffman, C. Beneking, in *Proceedings of 19th European Photovoltaic Solar Energy Conference* (2004)
41. S. Dubey, J.N. Sarvaiya, B. Seshadri, Energy Procedia **33**, 311 (2013)
42. J. Zhao, A. Wang, S.J. Robinson, M.A. Green, Prog. Photovolt: Res. Appl. **2**, 221 (1994)
43. N. Martin, J.M. Ruiz, Sol. Energy Mater. Sol. Cells **70**, 25 (2001)
44. D. Dirnberger, G. Blackburn, B. Müller, C. Reise, Sol. Energy Mater. Sol. Cells **132**, 431 (2015)


**Cite this article as**: Christos Monokroussos, Yating Zhang, Eleanor W. Lee, Frank Xu, Allen Zhou, Yichi Zhang, Werner Herrmann, Energy performance of commercial c-Si PV modules in accordance with IEC 61853-1, -2 and impact on the annual specific yield, EPJ Photovoltaics **14**, 6 (2023)